RAL-TR-95-041
Copy 2

CCLRC Library &
C4059437

RAL-P-95-
RAL TR - 95

CLRC

The Broad Emission-line Region in AGNS and Quasars: The Impact of Variability Studies

P M Gondhalekar M R Goad and P T O'Brien

LIBRARY
- 2 NOV 2010
RUTHERFORD APPLETON
LABORATORY

LIBRARY, R
-4 OCT 1995
RUTHERFORD APPL
LABORATORY

August 1995

COUNCIL FOR THE CENTRAL LABORATORY OF THE RESEARCH COU

The Central Laboratory for the Research Councils
Library and Information Services
Rutherford Appleton Laboratory
Chilton
Didcot
Oxfordshire
OX11 0QX
Tel: 01235 445384 Fax: 01235 446403
E-mail library@rl.ac.uk

ISSN 1358-6254

Neither the Council nor the Laboratory accept any responsibility for loss or damage arising from the use of information contained in any of their reports or in any communication about their tests or investigations.

THE BROAD EMISSION-LINE REGION IN AGNS AND QUASARS: THE IMPACT OF VARIABILITY STUDIES

P.M. GONDHALEKAR
Rutherford Appleton Laboratory Chilton, OXON., OX11 0QX.
M.R. GOAD
STScI, 3700 San Martin Drive, Baltimore, MD 21218, USA.
and
P. T. O'BRIEN
Astrophysics, Department of Physics, Keble Road, Oxford, OX1 3RH.

Abstract. Coordinated observations of variability of the continuum and the emission-line luminosities (reverberation mapping) in AGNs and quasars have fundamentally altered our understanding of the broad-line region in active galaxies. The constraints these observations impose on the models of the BLR have been demonstrated here by an attempt to model the BLR of NGC5548, the most intensively monitored AGN. Two models, a power law BLR and a Gaussian BLR, have been described and the modelled line luminosities and centroid of the line response functions are presented. A self-consistent model is presented for the change in the C IV/Lyα ratio as the continuum luminosity changes. It is shown that BLR gas must be composed of a mixture of optically thin and optically thick gas and the proportion of thick and thin gas alters with the luminosity of the ionizing continuum. The observed centroid or the lag of a line, can be a function of the continuum luminosity.

The variability of the profile of the C IV line in the spectrum of NGC5548 is investigated. This profile is extremely robust and is not significantly affected by changes in the ionizing continuum. Future models of the kinematics of the BLR clouds will have to consider very stable cloud motions and include anisotropic line emission.

AN HISTORICAL PERSPECTIVE

The International Ultraviolet Explorer (IUE) was launched on 26 January 1978 to herald a new era in astronomy at ultraviolet (1200Å to 3200Å) wavelengths. IUE was conceived at the then Astrophysics Research Unit (of the then Science and Engineering Research Council) and University College London. The full story of how a small observatory satellite planned in the UK became the International Ultraviolet Explorer, a joint US/ESA/UK project has not yet been told and it is not the purpose of this paper to tell this story. Here we recall the irritating regularity with which some of us, who worked on the IUE detectors, had to reiterate to the astronomical communities (on both sides of the Atlantic) that IUE was going to be capable of first rank extragalactic astronomy. The general perception was that IUE would perhaps be able to observe 3C273 and NGC 4151 and it would be nothing short of a miracle if any other extragalactic object was detected. No amount of gymnastics with pre-launch data would convince these sceptics that objects at a redshift of one were entirely within the grasp of IUE. How-

Astrophysics and Space Science 1995

Festschrift for Sir Robert Wilson, Professor Emeritius, University College London, UK.

ever, IUE confounded these sceptics, quasars around a redshift of two have been detected above 3σ level in the continuum. The observations of the double quasar Q0957+561 A,B (Gondhalekar & Wilson 1980) established IUE as an instrument which was making significant contributions at the forefront of modern extragalactic astronomy.

Soon after the in-flight verification phase, Professor R Wilson (UCL) suggested that the European astronomers with IUE time allocated for extragalactic observations should pool part of their allocations to undertake an intensive study of one or two active galaxies or quasars. This led to the founding of the European Extragalactic Collaboration (EEC) which in its early days was organised and coordinated by P M Gondhalekar (RAL). This collaboration decided to undertake a number of observations of 3C273, NGC 4151 and NGC 1068. The last object had to be dropped as it was not observable with IUE from the European (VILSPA) tracking station. The spectra of 3C273 were combined to produce a high signal-to-noise ratio spectrum (Ulrich et.al. 1980). But the observations of NGC 4151 produced the real surprise. This object was found to be violently variable over short time scales (Penston et.al. 1981). The large aperture of IUE and the absence of interfering atmosphere left no doubt that the observed variations were intrinsic to this Seyfert galaxy, and the rest, as they say, is history.

1. Introduction

Active galactic nuclei (AGNs) and quasars are the most luminous compact objects in the Universe. The generic model of these nuclei consists of a central super-massive object – probably a black hole (but a super-massive star burst has also been proposed) – surrounded by an accretion disc. This centre is embedded in three principal emission-line regions. The outermost region, the Extended Narrow Line region (ENLR), has an electron density of $\sim 10^3$ cm^{-3}, the spectral lines formed in this region have Doppler widths of $\sim 10^2$ km s^{-1}, and the radius of this region is ~ 10 kpc. The next region, the Narrow Line Region (NLR), has an electron density of $\sim 10^5$ cm^{-3}, line widths of $\sim 10^3$ km s^{-1}, and a radius of ~ 1 kpc. The inner-most region, the Broad Line Region (BLR), has electron densities $> 10^9$ cm^{-3} and emission-line widths of $\sim 10^4$ km s^{-1} (Netzer 1990, Osterbrock 1993). Both the ENLR and NLR can be spatially resolved in nearby AGNs, but the spatial structure of the BLR cannot be resolved with either existing or proposed astronomical instrumentation.

The BLR, lying closest to the central engine, is the least well understood. Early models of this region were largely concerned with establishing the basic ionization mechanism and an order-of-magnitude chemical composition (Bahcall and Koszlovsky 1969; Davidson 1972; MacAlpine 1972).

These early generations of models established that photoionization was the principle energy source, the clouds producing the lines were narrow filaments and these clouds have (broadly) solar composition (see the review by Davidson and Netzer 1979). For simplicity, and because observations demanded no better, the models assumed a single population of clouds, in a spherical geometry, to be responsible for all emission-line properties. These photoionization models suggested that the size of the BLR in AGNs is $\sim$0.1 pc and that in quasars is $\sim$1.0 pc.

The observations of correlated variability of luminosities of emission lines and the ultraviolet/optical continuum (line reverberation mapping) has brought about a profound re-appraisal of the models of the BLR. Only a few low-luminosity AGNs have been monitored in detail at present (see the reviews by Peterson 1993, 1995; Robinson 1995; and Maoz 1995 for details) and the BLR size, inferred from the time lag between the continuum and line variations, is at least a factor of ten smaller than that deduced from photoionization models. Moreover, these variability studies have demonstrated that the responsivity of the BLR clouds is radially stratified, such that the response of the low-ionization lines (LILs) (*e.g.* Mg II, Fe II, Hβ) originates from larger distances from the central source than the response of the high-ionization lines (HILs)(*e.g.* O VI, Lyα, C IV). The considerably smaller BLR sizes suggested by line reverberation studies implies that the BLR clouds in AGNs and quasars are exposed to a far more intense radiation field than had been previously considered. The implications of this enhanced radiation field have been considered by Ferland and Persson (1989). The high radiation fields would also suggest that a fraction of BLR clouds would be be optically thin and the spectrum of an *ad hoc* combination of optically thin and optically thick gas has been investigated by Shields *et.al.* (1995).

Despite this increased understanding of the physical state of the gas in the BLR many aspects of emission-line variability are poorly understood. Considerable emphasis has been placed recently on the interpretation of the line response functions (Blandford & McKee 1982, Horne *et.al.* 1991, Krolik *et.al.* 1991) recovered from variability monitoring data (a full discussion of the response function is given in Section 3). However, implicit assumptions made to recover the response function are poorly understood and do not necessarily reflect the realities of the physical state of the BLR gas. Also, the inversion provides *a* response function of a line, which is not necessarily *the* response function of a line. Moreover, the current quality of the monitoring data (*i.e.* sampling frequency, signal-to-noise, length of the light curves *etc.*) is such that the recovered response function is more a reflection of the inadequacies of the data and not the physics of the BLR. At present it is perhaps more fruitful to model the BLR and challenge these models with *all* data and parameters which result from the monitoring campaign and attempt to constrain the parameter space of the BLR. This approach has

the added advantage that the BLR parameters can be directly related to the observed light curves or the measured parameters. In this paper two models of the BLR are proposed and the output from these models is compared with the variability data on NGC5548, at present the most intensively monitored AGN. It is not the purpose of this paper to present a 'complete and final' model of the BLR in NGC5548 because this is not possible at present, instead this paper describes the constraints imposed by the reverberation studies on the proposed and future models of the BLR in this AGN.

An intensive monitoring campaign of NGC5548 was undertaken in 1989: this AGN was observed every four days for eight months with *IUE* and various ground-based telescopes. The bench-mark data, analysis and results obtained during this monitoring campaign have been presented by Clavel *et.al.* (1991), Peterson *et.al.* (1991), Dietrich *et.al.* (1993) Maoz *et.al.* (1993). A further short *IUE*/*HST*/optical campaign was conducted in 1993 and the results of this campaign have been presented by Korista *et.al.* 1995. These monitoring campaigns have provided very accurate data on line luminosities and the lag of a line *i.e.* the phase shift between the continuum and the emission-line light curves and also the centroid of the cross-correlation function of the ultraviolet continuum and line light-curves. The mean values of line luminosities and centroids are given in Table 1.

At present only the variability of the integrated line intensities to a change in the ionizing (as measured by the change in the ultraviolet/optical) continuum has been addressed (see reviews by Peterson 1993,1995). However, there is a considerable amount of convolved information locked in the profiles of emission lines, in particular, the kinematics of the radiating clouds can only be inferred from changes in the line profile. The profile variability has not received a great deal of attention up to now. A brief analysis of the variability of the profile of C IV line in NGC5548 is also presented in this paper.

The plan of this paper is as follows: In section 2 a mean continuum energy distribution (CED) of NGC5548 is derived; this CED is based on observations, where available. In subsequent sections this CED is used to model the photoionization of gas in the model BLRs. In Section 3, two BLR models with different spatial structures have been described and their model line luminosities and response function centroids are presented. The variation in the C IV/Lyα ratio as a function of continuum luminosity, is also modelled. In Section 4 the C IV line profile (the strongest and the best observed emission line in the spectrum of NGC 5548) and its variability behaviour have been investigated. The summary and conclusions are given in Section 5.

TABLE I

Observed and Modelled Line Luminosities and Centroids of NGC5548

Observed			Model F				Model G			
			$n = 10^{11}$ cm^{-3}		$n = 10^{12}$ cm^{-3}		$n = 10^{11}$ cm^{-3}		$n = 10^{12}$ cm^{-3}	
Line Id	R	τ^a_{cent}	R	τ_{cent}	R	τ_{cent}	R	τ_{cent}	R	τ_{cent}
O VI λ1035			1.18	7	1.30	3	1.57	8	0.48	7
Lyα λ1215	1	11.5	1.0	24	1.0	17	1.0	10	1.0	11
O V λ1218			0.16	11	0.23	3	0.25	8	0.13	7
N V λ1240	0.11[b]	6.5	0.21	12	0.48	5	0.28	8	0.31	7
Si IV λ1397			0.07	27	0.16	13	0.05	8	0.16	10
O IV λ1402			0.08	16	0.07	5	0.10	9	0.08	8
C IV λ1549	0.93[b]	12.0	1.06	24	0.92	10	1.18	10	1.32	10
He II λ1640	0.12[b]	5.0	01.7	16	0.29	11	0.27	9	0.24	9
Si III] λ1893			0.02	39	0.02	20	0.01	5	0.02	11
C III] λ1909	0.18[b]	28.5	0.03	20	0.01	9	0.03	7	0.02	9
Mg II	0.18[d]		0.05	49	0.09	39	0.01	9	0.04	10
Hγ	0.05[e]	16.5	0.01	29	0.02	30	0.01	10	0.01	10
He II λ4686	0.04[e]		0.02	15	0.04	12	0.02	9	0.03	9
Hβ	0.11[c]	21.5	0.03	30	0.05	33	0.02	10	0.03	10
He I λ5876	0.03[e]	14.0	0.02	26	0.03	23	0.01	10	0.02	9
Hα λ6563	0.41[e]	20.5	0.08	30	0.10	37	0.05	11	0.05	11
log(Lyα)	42.63		42.42		42.33		42.75		42.75	

τ_{cent}	line centroid (lt-days).
[a]	Peterson (1995)
[b]	Korista *et.al.* (1995)
[c]	Peterson *et.al.* (1991)
[d]	Clavel *et.al.* (1991)
[e]	Dietrich *et.al.* (1993)
R	Ratio of the line luminosity relative to the luminosity of the Lyα line.
log(Lyα)	Luminosity of the Lyα line (erg s^{-1}).

2. The Continuum Energy Distribution of NGC5548

A mean 'AGN continuum' has been described by Mathews and Ferland (1987) and has been extensively used to model the photoionization of gas in AGNs. However, observations in the soft X-ray and gamma-ray regions made since 1987 can be used to redefine the 'AGN continuum' in a form which would be more appropriate to model the BLR in NGC5548. Simultaneous *IUE* and *ROSAT/PSPC* observations of NGC 5548 have been presented by Walter *et.al.* (1994). These authors describe the observed CED from about 4 eV ($\sim$ 3000Å) to $\sim$ 10 keV by a parametric relation of the form $F_\varepsilon \sim \varepsilon^{(1-\Gamma_{UV})} \times exp(\varepsilon/\varepsilon_{cut}) + \varepsilon^{1-\Gamma_X}$ where Γ_{UV} is the ultraviolet spectral slope, Γ_X is the X-ray spectral slope and ε_{cut} is the cut-off energy in the EUV/soft X-ray. Unfortunately simultaneous hard X-ray (*Ginga*) observations were not available. However, in an extensive study of the hard X-ray (2 keV to 10 keV) emission from Seyfert 1 galaxies, Turner & Pounds (1989) have shown that $\Gamma_X = 1.9$ in most Seyfert 1 galaxies including NGC5548 and this slope of hard X-rays has been used here. The hard X-ray spectrum was normalized to the 2 keV flux detected by *ROSAT*. This hard X-ray spectrum with an ultraviolet slope $\Gamma_{UV} = 2.2$ and a cut-off energy ε_{cut}= 415 eV were assumed to define the continuum energy distribution of NGC 5548 from $\sim$ 3000Å to 10 keV.

Recent observations by the *Compton Observatory* have considerably increased our knowledge of the gamma-ray emission from AGNs and no Seyfert 1 galaxy has been found to have emission above 500 keV. The strongest emission has been observed from the Seyfert galaxy NGC 4151 and this spectrum falls off exponentially with an e-folding energy of 39 keV between 65 keV and 500 keV (Jourdain *et.al.* 1992). The shape of the gamma-ray spectrum of NGC 5548 was assumed to be similar to the observed spectrum of NGC 4151 and this was normalised to the hard X-ray power law spectrum extrapolated to 65 keV. The *IUE*, *ROSAT*, hard X-ray and gamma-ray spectrum of NGC 5548 is shown in Fig. 1. The crosses in Fig. 1 are the observed fluxes of NGC 4151. The lower flux of NGC5548 is consistent with the upper limits obtained by the *Compton Observatory*. The location of the source of gamma-rays in AGNs is unknown and it is not at all clear if the BLR in an AGN 'sees' the observed gamma-rays; the gamma-ray flux shown in Fig. 1 should be considered an upper limit of the flux which the BLR clouds would see if the gamma-rays in NGC5548 originate close to the central engine. Compared to the 'AGN continuum', the gamma-ray spectrum of NGC 5548 falls off very fast and the Compton heating due to gamma-rays will be considerably lower than that assumed in the past.

In the optical/near infra-red region ($\sim$ 3000Å to 1 μm) a power-law spectrum ($f_\nu \propto \nu^\alpha$) with a power-law index $\alpha = -1.0$ was assumed and this is compatible with observations (Neugebauer *et.al.* 1979). The continuum

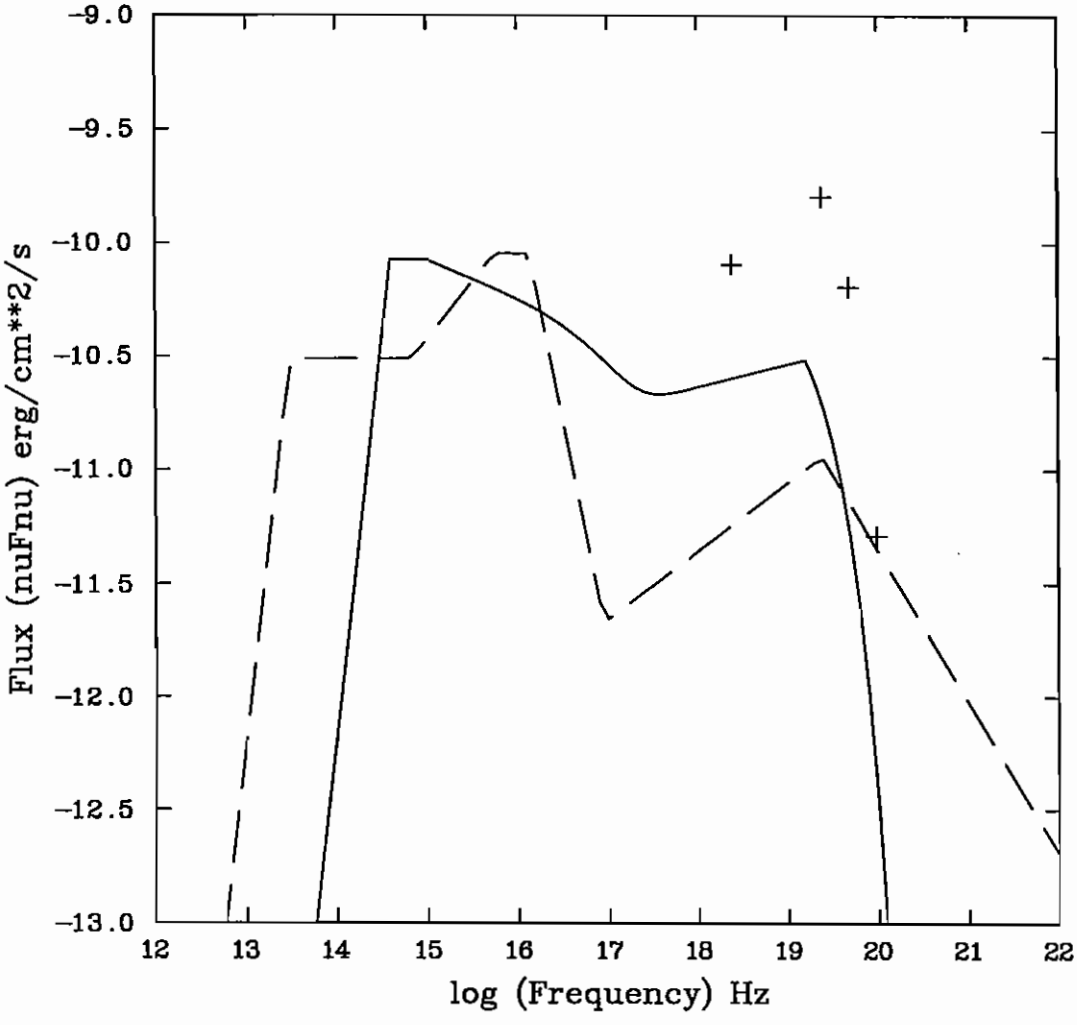

Fig. 1. Continuum Energy Distribution of NGC5548 (*full line*). The dashed line is the 'AGN Continuum' and the crosses are the gamma-ray observations of NGC4151

spectrum in the sub-millimetre region of radio quiet AGNs is poorly determined and the frequency at which the infrared spectrum turns over is not well known. A power-law radio spectrum with $\alpha = +2.5$ was assumed here and this is appropriate for self-absorbed synchrotron emission. The energy of the sub-millimeter break in the continuum has a major effect on the line ratios as the free-free heating will alter with this break. Ferland *et.al.* (1992)

have investigated the change in C IV/Lyα and O VI/Lyα ratios when the radiation field at ionizing energies and the density are held fixed but the frequency of the sub-millimetre break is varied. For the models presented here a sub-millimetre break at 1μm is assumed.

The lack of internal soft X-ray absorption (Walter *et.al.* 1994) suggests that the BLR clouds 'see' essentially the observed CED of NGC5548. The flux of ionizing photons, obtained by integrating the continuum from 13.6 eV to 2 keV, is 2.62 ph cm^{-2} s^{-1} . The mean intensity of Lyα (Clavel *et.al.* 1991) is 0.467 ph cm^{-2} s^{-1}. This suggests a covering factor of the BLR clouds of 0.18, assuming all the ionizing photons are converted to Lyα photons. The error in this covering factor is at least 15% due to the error in the intensity of the Lyα line. This is a lower limit as the error in the flux of ionising photons has not been included, although this is not expected to be greater than 20%. Moreover, the interpolated EUV spectrum (from ~11 eV to 200 eV) may not be the true EUV spectrum of NGC5548.

3. Models of the Broad Emission-Line Region

Over the last two decades a generic single-slab model of the BLR has been developed and discussed extensively (Davidson & Netzer 1979, Kwan & Krolik 1981, Ferland & Persson 1989). In this model the BLR clouds were assumed to be at a characteristic distance r from a central, single, isotropically emitting source of ionizing radiation. The geometry of the BLR was assumed to be spherical and the line emission from the clouds was also isotropic. The emission from this BLR is mainly a function of a dimensionless ionization parameter

$$U = \frac{Q(H)}{4\pi r^2 nc} \tag{1}$$

where $Q(H)$ is the luminosity of the central source (photons s^{-1}) and n is the electron density in the BLR clouds. These models assumed that a single population of clouds was responsible for all emission properties and large column densities were necessary to produce large optical depths in the Lyman continuum. These models failed to reproduce both the HILs and LILs from the same ensemble of clouds and thus prompted the introduction of two-component models (Collin-Souffrin *et.al.* 1986).

These early models considered the microphysics of the BLR (atomic physics, radiative transfer *etc.*) in great detail but almost no attention was paid to the macrophysics (*e.g.* geometry, spatial structure *etc.*). Future progress in modelling the BLR is clearly going to be in developing this understanding of the macrophysics of the BLR. Models of extended and stratified BLRs have been introduced by Rees, Netzer and Ferland (1989, hereafter RNF). These authors assumed a spherical geometry and a simple pressure

law to describe the radial distribution of BLR parameters and photoionization of BLR clouds by a single central source. The clouds were assumed to emit isotropically and the line and continuum emissivity from all parts of the BLR was integrated to obtain luminosities. However, these authors did not consider the response of this BLR to a change in the ionizing continuum. A parametric study of an extended BLR has been made by Pérez, Robinson and de la Fuente (1992a,b), who assumed a power-law radial distribution of line emissivity and investigated the response of an extended BLR of various radial structures and geometries. Goad, O'Brien and Gondhalekar (1993) (Paper I) and Goad (1995) have undertaken a detailed study of the response of an extended photoionized BLR. These authors assumed a pressure law and a radial distribution of BLR parameters, similar to that assumed by RNF, and proceeded to determine the luminosities and response functions of prominent emission lines and continua observed in the spectra of AGNs and quasars. O'Brien, Goad and Gondhalekar (1994) (Paper II) and Goad (1995) advanced this study to include anisotropic emission from clouds and O'Brien, Goad and Gondhalekar (1995) (Paper III) and Goad (1995) extended this study further to include the non-linear response of a stratified BLR.

The passage of an ionization front through a radially extended BLR can be described by a time-lag $\tau = (r/c)(1 - \cos\theta)$ where (r,θ) define the position of a cloud in the BLR, r is the radial distance from the source and θ is the angle between the cloud radius vector and the line of sight to a distant observer, measured from the side nearest to an observer. The clouds which respond to a continuum event after a time-delay τ lie on a parabolic surface of constant delay τ. The emission-line light curve $L(t)$, produced by an ionizing continuum light curve $C(t)$ passing through the BLR, can be described by the expression

$$L(v,t) = \int_0^\infty \Psi(v,\tau) C(t-\tau) d\tau \,, \tag{2}$$

where $\Psi(v,\tau)$ is the BLR 'response function', the response of an emission line as a function of delay τ, to a δ-function continuum event. The response function depends not only on the geometry and kinematics of the BLR but also on the observed line emissivity which is itself a function of the cloud location within the BLR, and the physical state of the gas at this location. In practice it is more common to measure the response of the integrated line flux to a continuum event whereby equation (2) reduces to

$$L(t) = \int_0^\infty \Psi(\tau) C(t-\tau) d\tau \,. \tag{3}$$

Equations (2) and (3) assume that there is a 'linear' relationship between the continuum and emission line variations (*cf.* paper III). The aim of reverberation studies of AGNs is to invert equation (2) (or equation (3)) to

determine the response function from the observed continuum and line light curves (Blandford & McKee 1982, Horne *et.al.* 1993). Stable solutions of this inversion are only possible for evenly sampled, high signal-to-noise ratio data obtained over long periods. With the amount and quality of data normally available it is more common to cross-correlate the time series $C(t)$ and $L(t)$ and determine the peak and the centroid of the cross-correlation function (CCF) (Gaskell & Sparke 1986, Gaskell & Peterson 1987, White & Peterson 1994). The peak delay is a measure of the time-of-flight from the continuum to the BLR and is, therefore, a measure of the scale length ($r = c\tau$) of the BLR (but see Perez, Robinson & de la Fuente 1992a,b). The centroid (τ_{cent}) of the CCF is equal to the centroid of the response function (Penston 1991, White & Peterson 1994). These statements depend very strongly on the assumption that the time-of-flight is the most significant time-scale in the response of the BLR to a continuum event and this has been established only for a few low luminosity AGNs (Peterson 1993,1995).

The centroid of the recovered response functions (*e.g.* Horne *et.al.* 1993) is equal to the responsivity and anisotropy weighted radius of the BLR, and is defined as

$$R = \frac{\int_{R_{in}}^{R_{out}} \eta(r) r L_{obs}(r,\theta) dr}{\int_{R_{in}}^{R_{out}} \eta(r) L_{obs}(r,\theta) dr}\,, \tag{4}$$

where $L_{obs}(r,\theta)$ is the observed luminosity and $\eta(r)$ is the responsivity of the BLR. The observed luminosity

$$L_{obs}(r,\theta) = 4\pi \int_{R_{in}}^{R_{out}} \varepsilon_{obs}(r,\theta) A_c(r) n_c(r) r^2 dr\,, \tag{5}$$

where the observed emissivity (Paper II)

$$\varepsilon_{obs}(r,\theta) = \frac{\varepsilon_{totl}(r)}{2}\{1 - (2F(r) - 1)\cos\theta\}\,, \tag{6}$$

where $\varepsilon_{totl}(r) = \varepsilon_{in}(r) + \varepsilon_{out}(r)$, $\varepsilon_{in}(r)$ is the emissivity of the inward cloud-face (facing the source) and $\varepsilon_{out}(r)$ is the emissivity of the outward cloud-face (away from the source). The anisotropy factor

$$F(r) = \frac{\varepsilon_{in}(r)}{\varepsilon_{totl}(r)}\,. \tag{7}$$

$F(r) = 0.5$ for an isotropically emitting cloud, whereas, $F(r) = 1.0$ for a fully anisotropically emitting cloud which emits only towards the source. This is a simple formalism for anisotropic line emission from BLR clouds, the actual form will depend critically on the shape of the clouds.

The responsivity of BLR clouds is defined as the fractional change in the cloud emissivity normalized to a unit fractional change in the ionizing

continuum, *for a small change in the ionizing continuum, i.e.*

$$\eta(\tau) = \frac{\delta\varepsilon(\tau)/\varepsilon(\tau)}{\delta U(\tau)/U(\tau)}, \tag{8}$$

where the change in the ionizing continuum has been represented by a change in the ionization parameter as the ionization parameter is linearly proportional to the ionizing continuum, assuming a fixed spectral shape. The implicit assumption here is that for a small change in the ionizing continuum the BLR clouds will respond linearly. This, of course, is not true for large continuum variations (see section 3.3). Non-linear response of a BLR has been discussed in detail in Paper III.

In this paper the luminosity and the centroid of the response functions of a few prominent lines have been determined for two models of the BLR. The two models differ in their radial distribution of the BLR parameters and are modelled with the code PROSYN (Goad 1995). A spherical geometry is assumed for both models. The cloud abundance was assumed to be solar (Grevesse & Anders 1989), this is consistent with the available data on Seyfert 1 galaxies (Hamann & Ferland 1993). The emissivities of the photoionized clouds were obtained from the code CLOUDY (version 84.12a, Ferland 1993). The CED of NGC5548 described in section 2 is used for these photoionization calculations.

3.1. A Pressure-Law Model

A pressure-law model of an extended BLR has an inner and an outer radius R_{in} and R_{out} respectively and is populated with spherical constant density clouds in pressure balance with the intercloud medium. A strict pressure balance between the BLR clouds and the intercloud medium appears unlikely (Mathews & Ferland 1987), although magnetic pressure may provide the additional support necessary to prevent cloud disruption (Rees 1987). Furthermore, this formalism has the added advantage of reducing the number of free parameters necessary to describe the model. The pressure is assumed to have a power-law radial dependence $P \propto r^{-s}$ and as the gas kinetic temperature is a weak function of U, the gas density $n(r) \propto r^{-s}$ and $U(r) \propto r^{s-2}$. Assuming that the mass of the clouds is conserved, the cloud cross-sectional area $A_c(r) \propto r^{2s/3}$ and the column density $N(r) \propto r^{-2s/3}$. Also assuming that the clouds move with their virial velocity, the differential covering factor $dC(r) \propto r^{(2s/3)-(3/2)}dr$. A pressure-law model is thus defined by the pressure-law index s, R_{in}, R_{out}, the density and the column density at the inner radius, the total covering factor and the luminosity and spectrum of the ionizing and heating continuum.

A model with pressure-law index $s = 0$ is considered here and thus will be referred to as model F. However, we note that the model F discussed

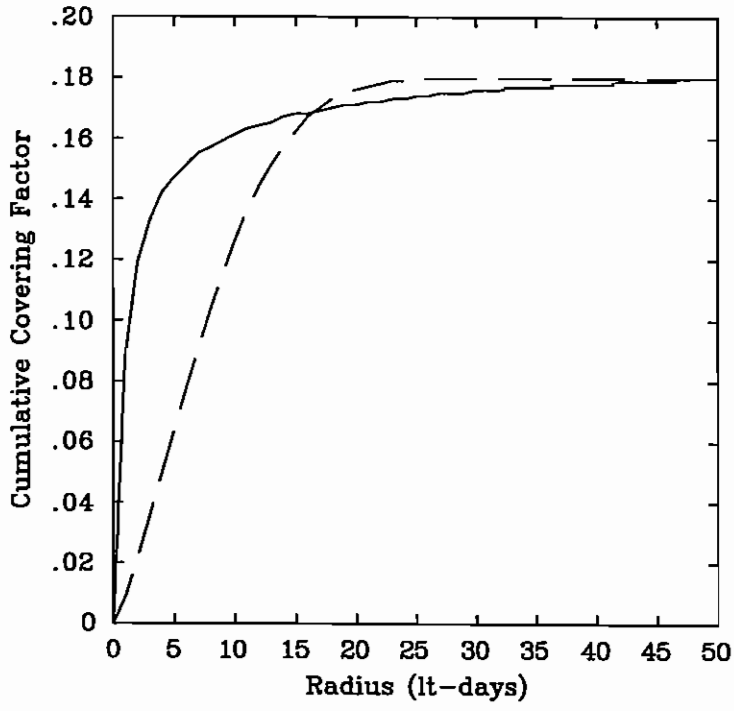

Fig. 2. Cumulative Covering Factor, for Model F (*full line*) and Model G (*dashed line*).

in papers I–III has $n = 10^{10}$ cm^{-3}. The inner radius of this BLR was set at 0.3 lt-days; this radius is large enough for the continuum source to be approximated by a point source. Also at this radius the relativistic effects of the central black-hole (if that is the central engine) will be negligible. The outer radius was set at 53 lt-days which conforms with the criterion defined by RNF, namely [O III] λ4363/Hβ< 0.1. A column density of 10^{23} cm^{-2} at R_{in} was assumed for this model, and for $s = 0$ the column density, of course, stays constant with radius.

The cumulative covering factor as a function of distance from the source is shown in Fig.2. The covering factor was normalized such that the integrated covering factor at R_{out} was equal to the measured covering factor of 0.18. The radial variation of the ionization parameter (for n=10^{11} cm^{-3} at R_{in}) is shown in Fig.3. At the inner radii the ionization parameter is larger than the values which have been considered for most models. For a column density of 10^{23} cm^{-2} the BLR clouds will be optically thin for an ionization parameter greater than 0.5, and in model F a large fraction of the inner BLR will be radiation bound.

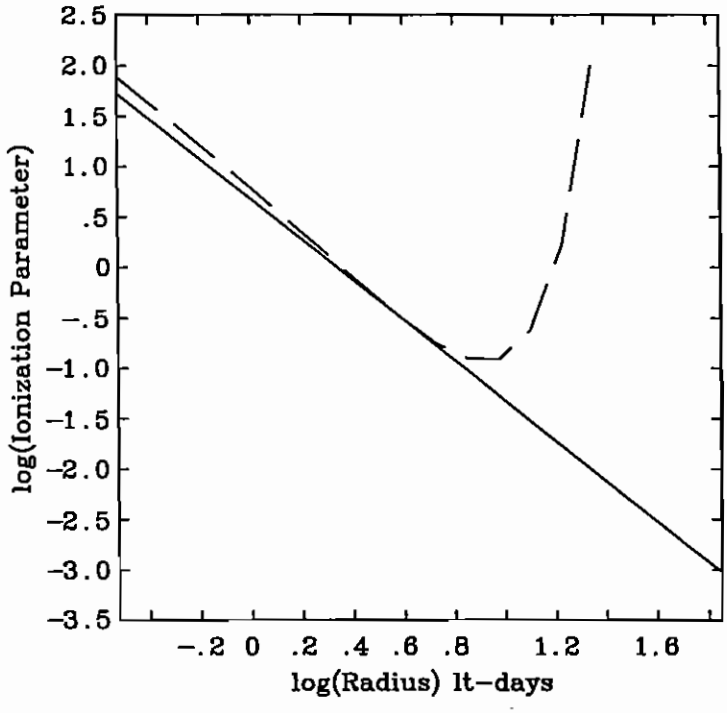

Fig. 3. Distribution of the ionization parameter as a function of the distance from the central source. Model F (*full line*), and Model G (*dashed line*).

The change with density, of the Lyα line luminosity in model F is shown in Fig.4. The luminosity of this line increases with density and peaks around $n = 10^{11}$ cm^{-3} although this peak luminosity is about 40% lower than the mean luminosity of NGC5548 measured during the 1989 monitoring campaign (Clavel *et.al.* 1991). Similarly, the change with density in the luminosity (relative to Lyα) of six lines is shown in Fig.5. In this model the luminosity of the O VI λ1035 line is exceptionally high as this line is emitted principally by the highly ionized gas at low radii. From equation (1), for a fixed $Q(H)$, $U \propto n^{-1}$. In model F as the density of the gas increases (*i.e.* U decreases), the emissivity at low radii increases (see Fig.6) and the total luminosity rises.

This can be seen more clearly in the luminosity of the N V λ1240 line, which rises very rapidly with density because the emissivity of the line at low radii increases with density. The emissivity of the C IV λ1549 line at low radii also increases with density, but the emissivity at larger radii drops and because the bulk of the gas is at the outer radii (Fig.2) the luminosity of the line falls slightly with increasing density. The luminosity of the

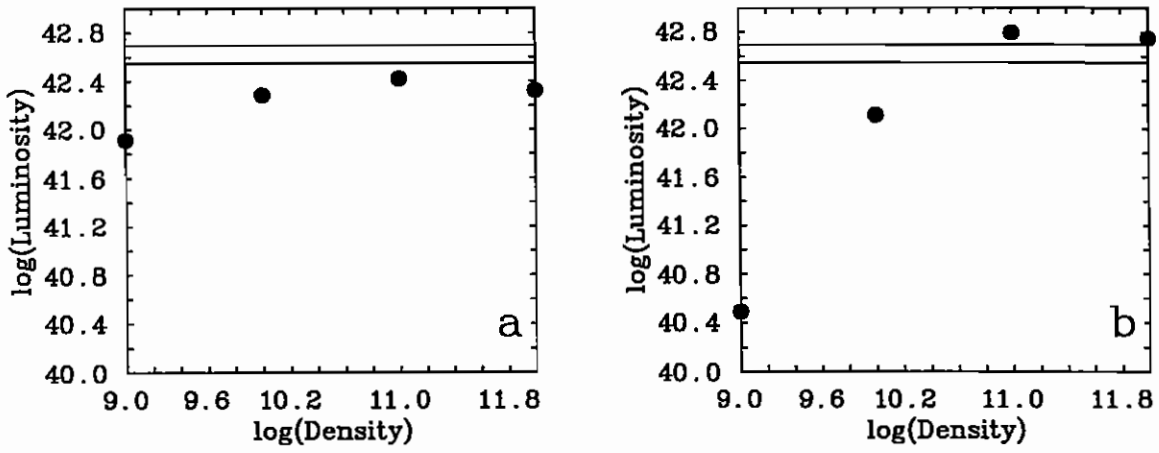

Fig. 4. The luminosity of Lyα line as a function of density, (a) Model F and (b) Model G. The two parallel lines indicate the upper and lower limit (1 σ) of observations made during the 1989 monitoring campaign of NGC5548.

He II λ1640 line also increases with density, but this is not entirely due to the increase in the emissivity at low radii. At higher densities this line becomes more isotropic (Fig.6) and, therefore, the observed luminosity increases. The luminosity of the C III] line drops with density as this line is collisionally de-excited at densities greater than $\sim 10^{10}$ cm^{-3}. The luminosity of the Hβ line is not very sensitive to density.

The change with density, in the centroid of the lines is shown in Fig.7. The centroid of all lines decreases with increasing density. This is due to the increase, at low radii, in the emissivity of a line as the density is increased (Fig.6) and also due to the increase in the responsivity of the lines, at the inner radii, as the density increases. This increase in responsivity will tend to push the centroid of a line to lower values.

The model F luminosity of the Lyα line and the relative (with respect to Lyα) luminosities of fifteen other lines are given in Table 1. The centroid of the response functions of these lines are also given in Table 1. The line luminosities have been given relative to the luminosity of the Lyα line only, but Model F suggests that the O V λ1218 line (and possibly the HeIIλ 1216Å line, whose luminosity has not been calculated here, but see Shields *et.al.* (1995)) could be strong and the observed line ratios could be measured relative to the luminosity of Lyα line blended with these two lines and the observed ratios would be lower than the modelled ratios. To estimate the strength of the O V λ1218 line a blend of the modelled Lyα and O V lines was produced; the profiles of these lines were assumed to be similar to the

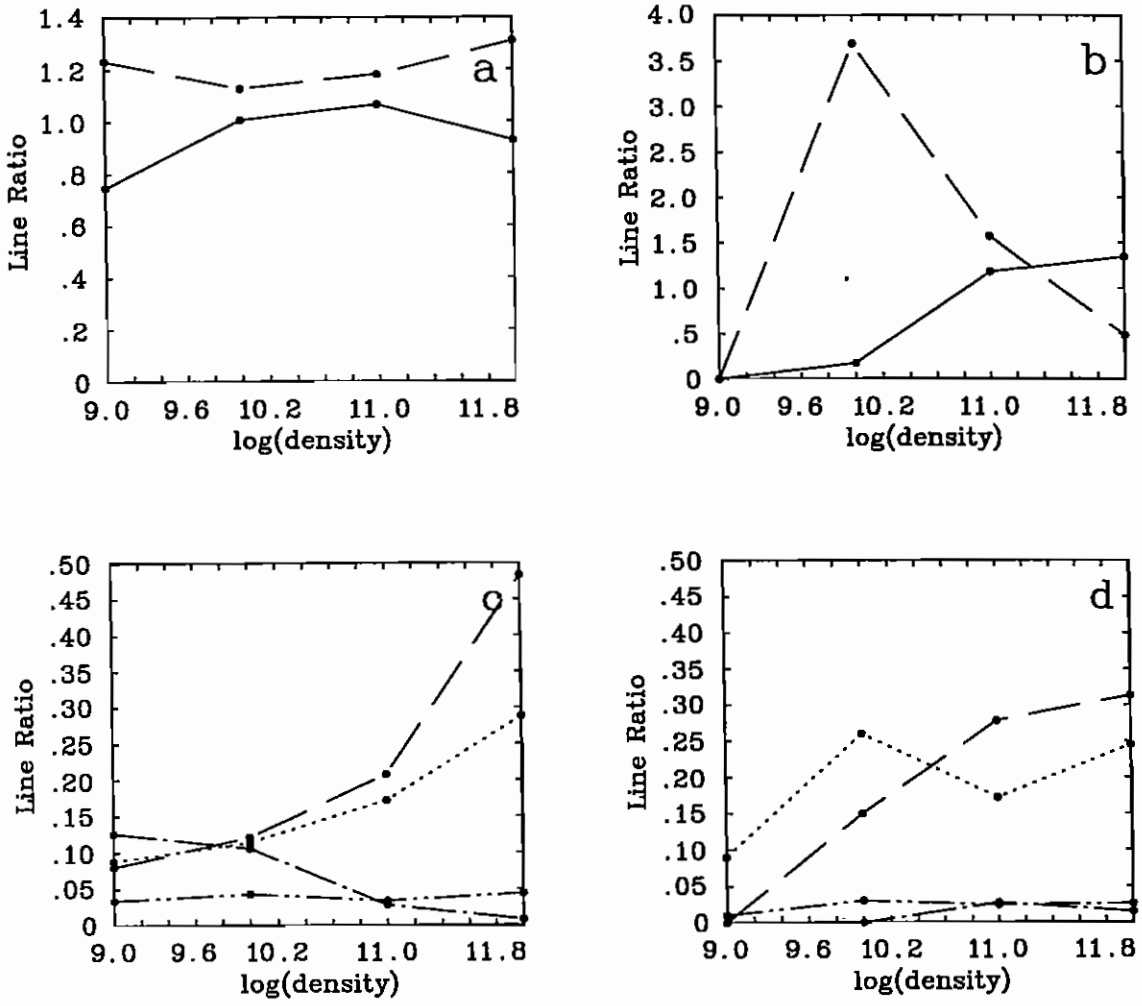

Fig. 5. The line luminosities (relative to Lyα) as a function of density in Model F (a,c) and Model G (b,d). In (a,b), *full line*-C IV and *dashed line*-O VI. In (c,d), *dashed line*-N V, *dotted line*-He II, *dot-dash line*-C III] and *dot-dot-dash line*-Hβ.

profile of the C IV λ1549 line but the integrated flux of the Lyα line was normalized to unity and that of the O V line was normalized to the modelled line ratio. This blend suggests that for O V/Lyα > 0.25 a shoulder would appear in the red-wing of Lyα and this would be resolved in the *HST/FOS* spectra. This shoulder is not seen in the *HST/FOS* spectra of NGC5548

(Korista *et.al.* 1995), suggesting that O V Lyα < 0.25. In practice it should be possible to detect O V line even weaker than that suggested by this lower limit of the line ratio because the Lyα line is narrower than the C IV line.

The model F line luminosities and centroids have been obtained for densities of 10^{11} cm^{-3} and 10^{12} cm^{-3} respectively. The line emissivity, responsivity and anisotropy factor for seven prominent lines are shown, for these two densities, in Fig. 6. As noted above the luminosity of the O VI line is high in this model. The luminosity of the O VI line in NGC 5548 is unknown but in AGN in general the O VI/Lyα+N V ratio is between 0.06 and 0.5 (Zheng *et.al.* 1995). From the data in Zheng *et.al.* the observed $\alpha_{ox} \sim 1$ for NGC5548 which implies O VI/Ly$\alpha \sim 0.4$. The strength of the N V line is also overestimated (by at least a factor of two) but the strengths of all other HILs are compatible with the observations. The strength of all LILs is underestimated by a large fraction; this problem is not new and is certainly not solved in a stratified BLR.

The model F centroids of all lines are higher than the observed centroids by at least a factor of two. This can be understood with reference to Fig. 6. The emissivities of all lines are low at the inner radii and the line responsivities are also low or negative, which will conspire to push the line centroids to higher values. When the density is increased to 10^{12} cm^{-3} the emissivity at inner radii increases and the responsivity at these radii also increases becoming positive for all lines. This will push the line centroids to lower values as can be seen from Table 1. However, at this higher density the luminosity of the N V line (and the O VI line) increases further although the line centroids are now in agreement with observations. The luminosities of other HILs are still compatible with observations but the luminosities of the LILs are still underestimated. In conclusion the model F line luminosities and centroids of HILs are in reasonable agreement with observations for a density of 10^{12} cm^{-3} but the model underestimates the luminosities of LILs and overestimates their centroids.

3.2. A Gaussian Model

In this model the density is expressed as

$$n_{\xi} \propto exp(-((r - r_p)/\sigma)^2 \tag{9}$$

Where r_p and σ (=FWHM/2.354) are respectively the radius of the peak and the standard deviation of the density distribution. Note that this is an *ad hoc* assumption and no physical mechanism is offered for this density distribution. In this sub-section the line emission from a spherical distribution of such gas and the response of this gas to a change in the ionizing radiation are investigated.

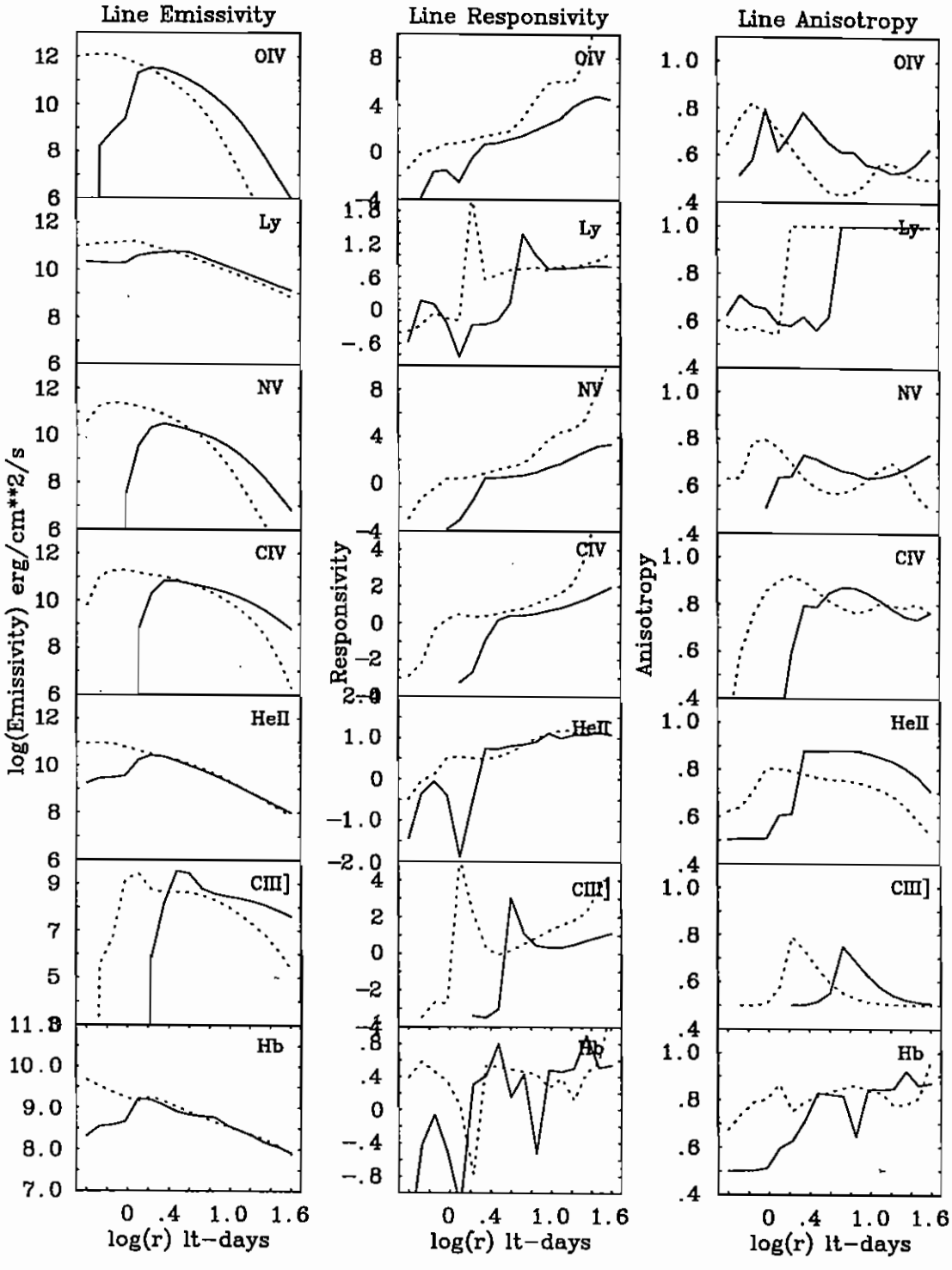

Fig. 6. The radial distribution of emissivity, responsivity and the anisotropy factor for Model F, at density $n = 10^{11}$ cm^{-3} (*full line*) and $n = 10^{12}$ cm^{-3} (*dotted line*).

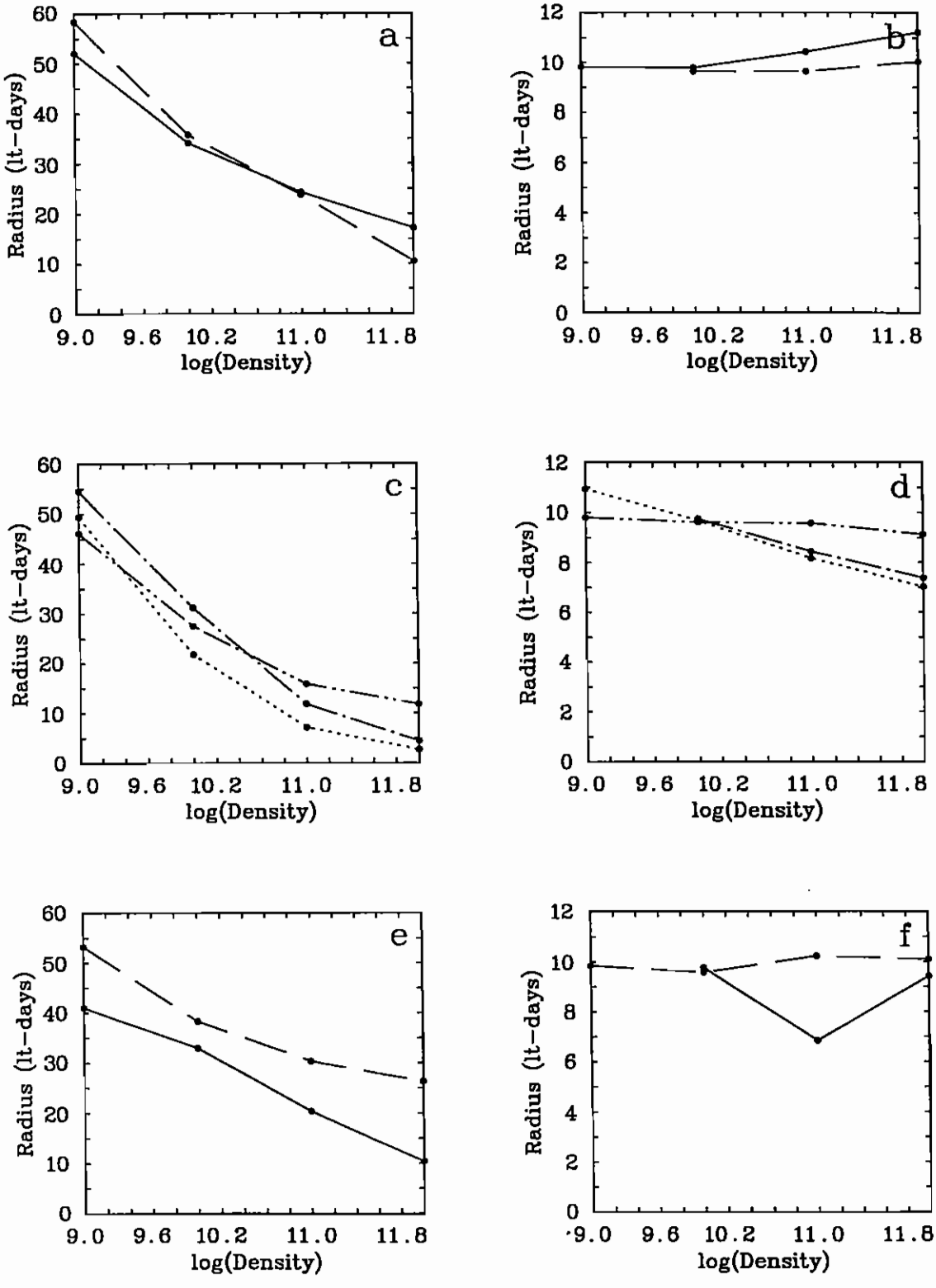

Fig. 7. Line centroids as a function of density, Model F (a,c,e) and Model G (b,d,f). In (a,b), (*full line*)-Lyα and (*dashed line*)-C IV. In (c,d), (*dotted line*)-O VI, (*dot-dash line*)-N V and (*dot-dot-dash line*)-He II. In (e,f), (*full line*)-C III] and (*dashed line*)-Hβ.

Assuming constant density spherical clouds of radius R_c and mass conservation

$$nR_c^3 = constant \tag{10}$$

The cloud cross-sectional area

$$A_c \propto R_c^2 \propto exp(2/3(((r - r_p)/\sigma)^2)) \tag{11}$$

The cloud column density

$$N = nR_c \propto exp(-2/3(((r - r_p)/\sigma)^2)) \tag{12}$$

The differential covering factor

$$dC(r) \propto A_c(r)n_c(r) \tag{13}$$

Where the cloud number density $n_c(r)$ is also assumed to have the same Gaussian distribution as the density

$$n_c(r) \propto exp(-((r - r_p)/\sigma)^2) \tag{14}$$

and

$$dC(r) \propto exp(2/3(((r - r_p)/\sigma)^2)) \times exp(-(((r - r_p)/\sigma)^2)) \tag{15}$$

The ionization parameter

$$U(r) \propto r^{-2} \times exp(((r - r_p)/\sigma)^2) \tag{16}$$

This model will be referred to as Model G. In this model the 'density' refers to the density at the peak of the density distribution. To obtain integrated line luminosities the inner radius R_{in} = 0.3 lt-days was assumed for reasons given in Section 3.1. The outer radius had to be truncated at 22.5 lt-days as beyond this radius the density drops to a level where meaningful computations cannot be made. This model is thus characterised by the inner and outer radii, R_{in} and R_{out} respectively, the peak (r_p) and the FWHM of the density distribution and the density and the column density at the peak of the distribution. The Model G described here is computed for r_p = 4 lt-days, FWHM = 10 lt-days, and a column density of 10^{23} cm^{-2} at r_p.

The cumulative covering factor for Model G is shown in Fig. 2. Compared to Model F there is less gas at low radii in model G. The radial dependence of the ionization parameter, calculated for a density of 10^{11} cm^{-3} is shown in Fig. 3. At low radii the ionization parameter is similar to the ionization parameter for Model F. At larger radii the ionization parameter rises steeply, due to the rapid drop in density, and as a consequence the gas at large radii will be heavily ionized.

The model G luminosity of the Lyα line as a function of density is shown in Fig. 4. The line luminosity rises very steeply with density and

peaks around 10^{11} cm^{-3}. The peak luminosity is about 32% higher than the mean luminosity of NGC5548 observed during the 1989 monitoring campaign (Clavel *et.al.* 1991). The relative luminosities of six prominent emission lines, as a function of density, are shown in Fig. 5. The luminosities of the O VI, N V, C IV and He II lines increase with density but that of O VI drops beyond a density of 10^{10} cm^{-3} and the luminosities of all other lines begin to flatten around 10^{11} cm^{-3}. This increase in line luminosities with density is due to an increase, with density, in the line emissivity at low radii (see Fig. 8.).

The line centroids, as a function of density, are shown in Fig. 7. The centroids of both the Lyα and C IV lines increase slightly with density because both lines become more anisotropic as the density increases and this pushes the centroid to higher values. The centroids of the O VI and N V lines, on the other hand, drop with increase in density. This happens because the responsivity of these lines at the inner radii, increases as the density rises and this tends to push the centroids to lower values. The centroids of He II and Hβ are unaffected by an increase in density because the increase with density in the responsivity of these lines at low radii, which would ordinarily decrease the value of the line centroids, is mitigated by the increasing anisotropy of the line emission at low radii. Similarly, the value of the centroid of the C III] line increases at 10^{12} cm^{-3} because the line emission becomes more anisotropic at lower radii as the density increases.

The model G luminosity and centroid of the Lyα line and the relative luminosities of fifteen lines and the centroids of these lines are given in Table 1. These line parameters have also been obtained for densities of 10^{11} cm^{-3} and 10^{12} cm^{-3} respectively. This model also predicts a strong O V λ1218 line and if this is blended with the Lyα line then the observed line ratios will be smaller than the modelled ratios. However, the *HST/FOS* spectra of NGC5548 suggest that model G also over-estimates the strength of the O V line. Similarly, this model over-estimates the strength of the O VI and N V lines, and the greater strength of these lines is mainly due to the emission from the highly ionized gas at the inner radii where the ionization parameter is high. The relative strengths of other HILs are compatible with observations, but even in model G the strengths of LILs are underestimated by a large fraction. The centroids of all HILs are in reasonable agreement with observations of these lines. But the centroids of LILs are underestimated by about a factor of two.

At a density of 10^{12} cm^{-3} the luminosities of all the HILs (except O VI) increases, mainly due to the rapid increase in the line emissivity at the inner radii. The centroids of most HILs decrease slightly at this higher density because the responsivity of the lines, at inner radii, increases with density and this tends to push the centroid to lower value. The centroid of the Lyα line, however, increases slightly with density because the line emission

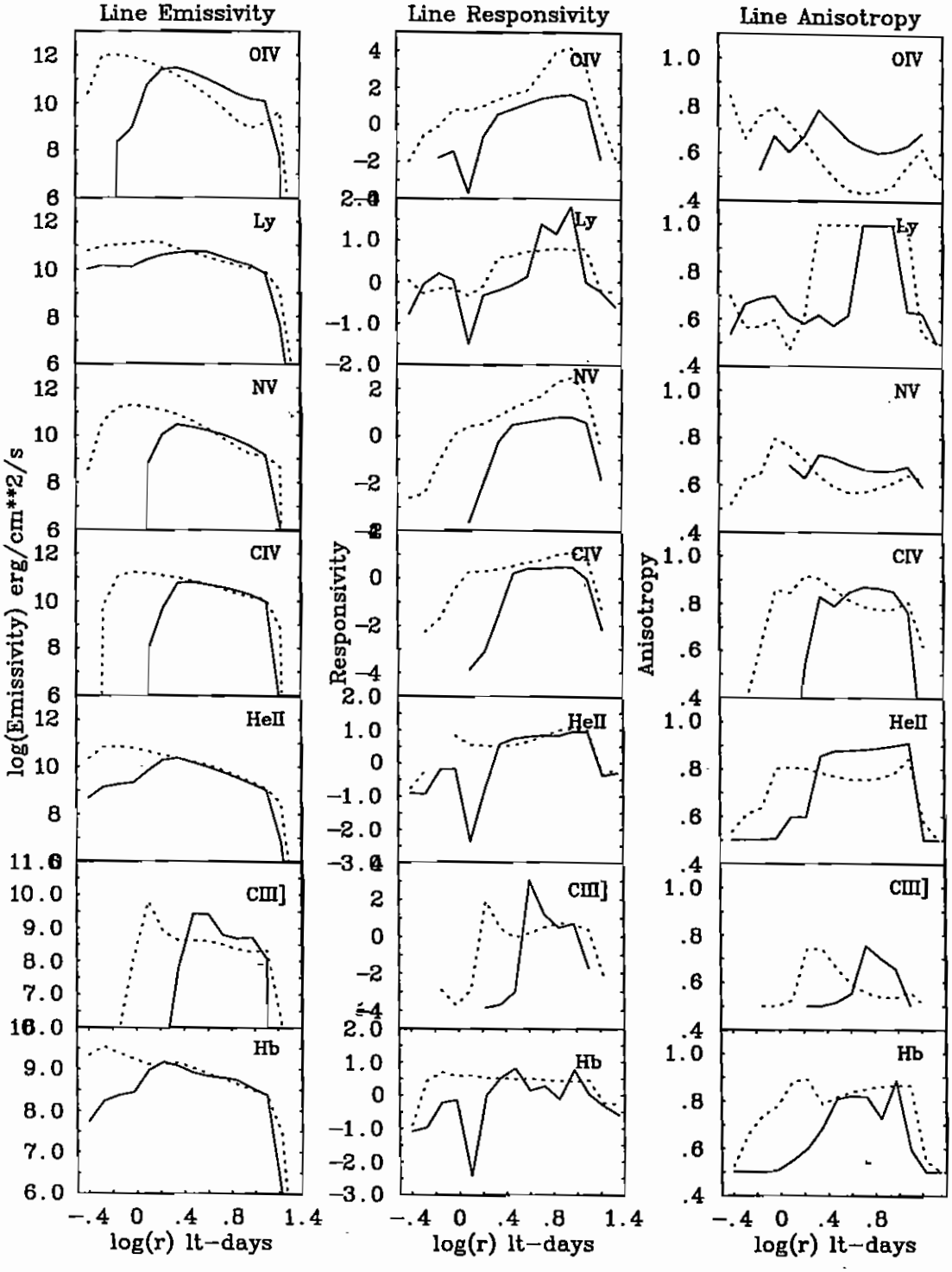

Fig. 8. The radial dependence of line emissivity, responsivity and the anisotropy factor for Model G, at density $n = 10^{11}$ cm^{-3} (*full line*) and $n = 10^{12}$ cm^{-3} (*dotted line*).

becomes anisotropic over a larger radial distance at this higher density. This is true of the C IV line as well but in this case the increase in the responsivity of the line at lower radii, which would tend to push the line centroid to a lower value, is balanced by the increase in the line anisotropy, over a larger radial region, which pushes the centroid to higher values.

3.3. The C IV/Lyα Ratio in NGC5548

Observationally it has been demonstrated that a negative correlation between the C IV/Lyα ratio and the continuum luminosity is a common occurence in variable Seyfert galaxies (Clavel & Santos-Lleó 1990, Kinney, Rivolo & Koratkar 1990, Pogge & Peterson 1992, Gondhalekar 1992). However, the single-slab photoionization models of the BLR predict that the C IV/Lyα ratio should remain constant or increase as the luminosity of the ionizing continuum increases. This lack of agreement between observations of two energetically significant lines and model predictions brings into sharp focus the inadequacy of the single-slab model of the BLR in AGNs.

The C IV/Lyα ratio is sensitive to the CED of the ionizing continuum (and the sub-mm break in the CED of AGNs). The negative correlation between this ratio and the continuum luminosity can be explained in terms of a changing shape of the ionizing continuum dominated by a soft excess (Binette *et.al.* 1989, Clavel & Santos-Lleó 1990, Gondhalekar 1992). However, Shields *et.al.* (1995) have questioned this explanation pointing out that there is growing evidence that a non-negligible fraction of the BLR cloud population is optically thin to the Lyman continuum and fully ionized in hydrogen, and thus a change in the relative proportion of optically thin and thick gas can explain the negative correlation between the C IV/Lyα ratio and the continuum luminosity. Shields *et.al.* illustrate this with an *ad hoc* combination of optically thin and thick gas.

The negative correlation of the C IV/Lyα ratio with continuum luminosity is re-examined here within the context of models F and G. In Fig. 9. the C IV/Lyα ratio in NGC5548 from the 1989 monitoring campaign (Clavel *et.al.* 1991) is plotted as a function of Lyα luminosity. The ratio has not been shown as a function of continuum luminosity, as has usually been done in the literature, because it is now known that there is a lag of about 10 days between a change in the continuum and a corresponding change in the Lyα and C IV lines. This lag will introduce additional scatter in the ratio/continuum correlation (Pogge & Peterson 1992). Also Lyα and C IV lines have been shown to form in the same region of the BLR and the correlation between the line ratio and the luminosity of the Lyα line refers to a well defined region of the BLR.

The C IV/Lyα ratio computed for model F, as the continuum luminosity is increased, is shown in Fig. 9. Note that the shape of the CED was not altered.

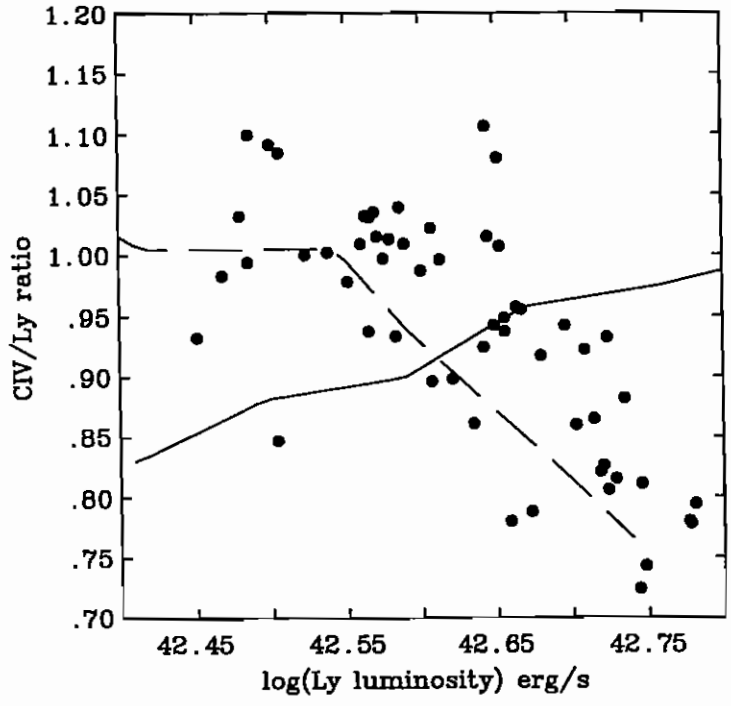

Fig. 9. The correlation between the C IV/Lyα ratio and the luminosity of the Lyα line in NGC5548. The *dots* are the data obtained during the 1989 campaign to monitor NGC5548. The *full line* represents Model F and *the dashed line* Model G.

The model line ratio and the luminosity of the Lyα line were obtained for a density of 10^{12} cm^{-3} and the luminosity had to be increased by 0.21 (in the log) to match the observed luminosity. The lack of agreement between the observations and the model can be understood by reference to Fig. 10. where the the luminosities of the Lyα and C IV lines have been shown as a function of continuum luminosity. As the continuum luminosity is increased in model F, the rate of increase of the luminosity of the C IV line is higher then that of the Lyα line and this results in an increase in the C IV/Lyα ratio. The line luminosities have been computed for slightly higher continuum luminosity than is required to model the observed C IV/Lyα ratio to demonstrate that in this model, the line luminosities do not saturate, unless of course the luminosity is increased to unrealistic levels.

The C IV/Lyα ratio computed for model G is also shown in Fig. 9. The luminosity of the Lyα line had to be decreased by 0.12 (in the log) and the C IV/Lyα ratio had to be decreased by 0.18 to bring the model into agreement with observations. However, this may just reflect the uncertainty in the

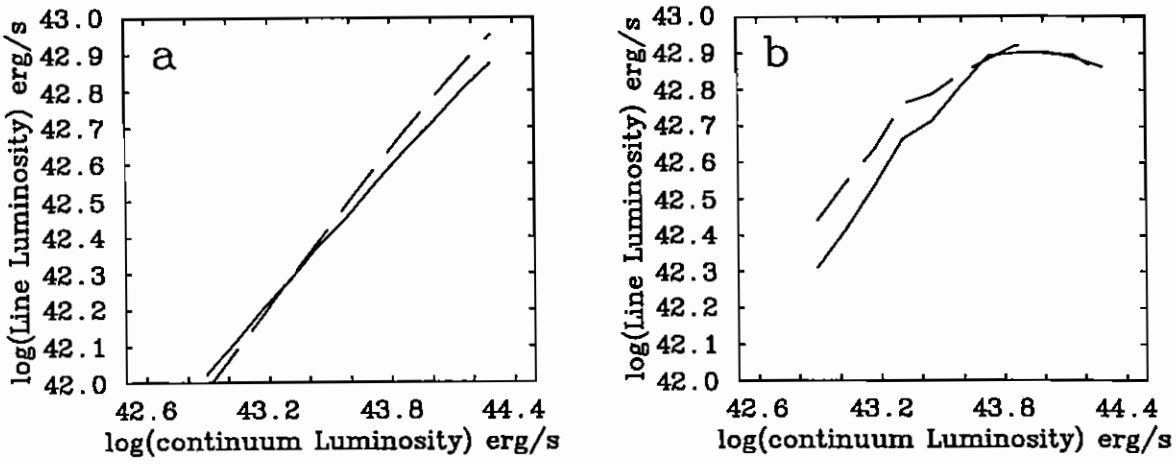

Fig. 10. The luminosities of the Lyα (*full line*) and C IV (*dashed line*) lines as a function of continuum luminosity, (a) Model F and (b) Model G.

cloud covering factor. Thus, although the trend in the modelled C IV/Lyα ratio is in very good agreement with observations, in absolute terms the general agreement is fairly poor. The model G luminosities of the Lyα and C IV lines, as a function of continuum luminosity, have been shown in Fig. 10. Relative to the rate of increase of Lyα luminosity, the rate of increase of C IV luminosity decreases as the continuum luminosity rises and this leads to a decrease in the C IV/Lyα ratio. It is interesting to note that at high continuum luminosities the line luminosities flatten, as has been observed for Fairall 9 (Wamsteker & Colina 1986). This is due to an increasing fraction of optically thin gas in the BLR as the continuum luminosity increases and eventually the BLR becomes radiation bounded, as has been claimed by Wamsteker & Colina (1986). The increase in the amount of optically thin gas with increasing continuum level provides a natural explanation for the observed behaviour of the C IV/Lyα ratio in NGC5548 and other AGNs.

The model F centroids of the Lyα and C IV lines, as a function of continuum luminosity, are shown in Fig. 11. The centroids increase by over a factor of three over the continuum luminosity considered. This increase can be understood by considering the emissivity, responsivity and the anisotropy factor of these two lines shown in Fig. 12. These line parameters are given for both low and high continuum levels. As the continuum luminosity increases the emissivity of Lyα at larger radii increases which leads to an increase in the luminosity of the line. The responsivity of the line at small radii decreases which tends to push the line centroid to higher values, although this is slightly mitigated by the line emission becoming more isotropic as

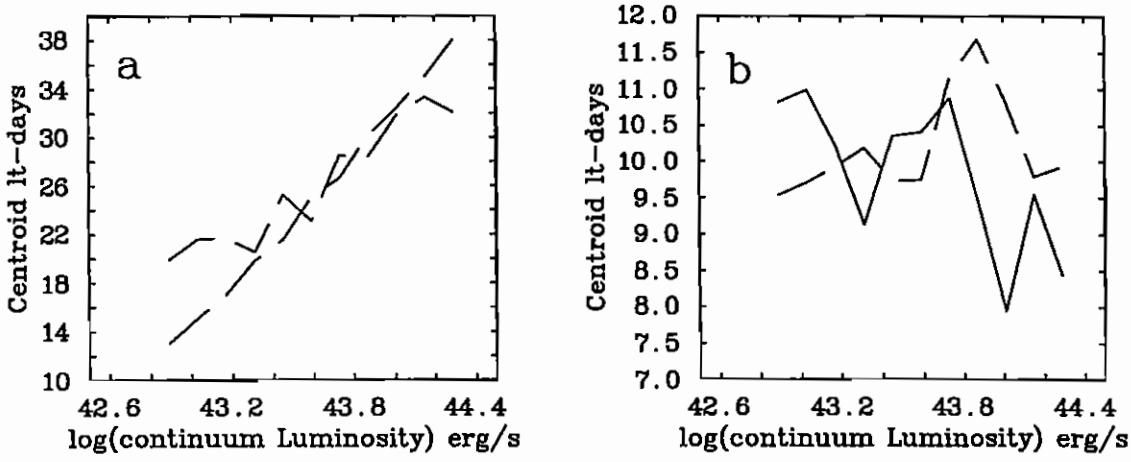

Fig. 11. The centroid of Lyα (*full line*) and C IV (*dashed line*) as a function of continuum luminosity, (a) Model F and (b) Model G.

the continuum luminosity rises. The C IV line behaves slightly differently. Although the line emissivity at small radii decreases as the continuum luminosity increases as C^{+3} ions are ionized to a higher state, the emissivity of the clouds at larger radii increases, and as more gas is concentrated at larger radii the line luminosity increases. The line responsivity at lower radii decreases as the continuum luminosity rises because more gas at the inner radii is ionized, and this pushes the line centroid to higher values. For a BLR similar to model F the line centroids, obtained from cross correlation of continuum and line light curves, would be a strong function of the history of continuum variability.

The model G centroids of the Lyα and C IV lines as a function of continuum luminosity, are also shown in Fig. 11. The centroid of Lyα drops from $\sim$11 lt-days to $\sim$8 lt-days as the continuum luminosity increases, however, the centroid of the C IV line is nearly constant (give or take a peak or a drop). This can also be understood by reference to model G line emissivity, responsivity and the anisotropy factor for these two lines shown in Fig. 13. As the ionizing continuum increases the Lyα line gradually becomes optically thin and the line emission becomes isotropic at all radii and this results in a gradual decrease in the value of the line centroid. The C IV emissivity at lower radii drops, because of ionization to a higher state, and the line becomes less anisotropic over a larger radial distance, but the expected drop in the value of the centroid is balanced by the decrease in the line responsivity at the inner radii, which tends to push the centroid to higher values. If the BLR of NGC5548 is similar to model G then the cross correlation

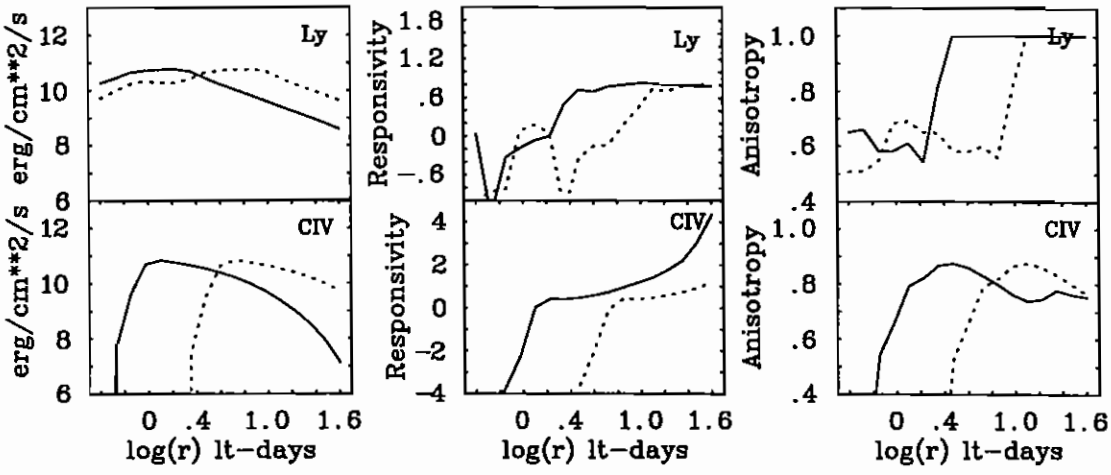

Fig. 12. The radial dependance of line emissivity, responsivity and the anisotropy factor in Model F. The (*full line*) data were obtained for low continuum luminosity and the (*dotted line*) data were obtained for high continuum luminosity.

of continuum and line light curves would result in values of line centroids which would be close to the centroid of line response functions and would not be a strong function of the continuum light-curve.

In conclusion, model G can reproduce the trend in the observed correlation between C IV/Lyα ratio and the continuum luminosity although it does slightly over-estimate the line ratio and the line luminosity.

4. The Profile of C IV Line

The kinematics of the BLR clouds is poorly understood. Both inflow and outflow have been suggested and random Keplerian orbits are equally likely. The profiles of emission lines are determined by the Doppler motion of the BLR clouds and information on cloud kinematics is convolved in these profiles. Most of the studies of line profiles have concentrated on the Hβ line (eg. Boroson and Green 1989) as this line is accessible to observations at high spectral resolution. However, the reverberation studies suggest that the Hβ line is formed a few tens of lt-days from the source of ionizing radiation and may not be formed in the ensemble of clouds which emit the Lyα and C IV lines. The profiles of these two lines have not been studied in any detail because of their relative inaccessibility to high-resolution observations

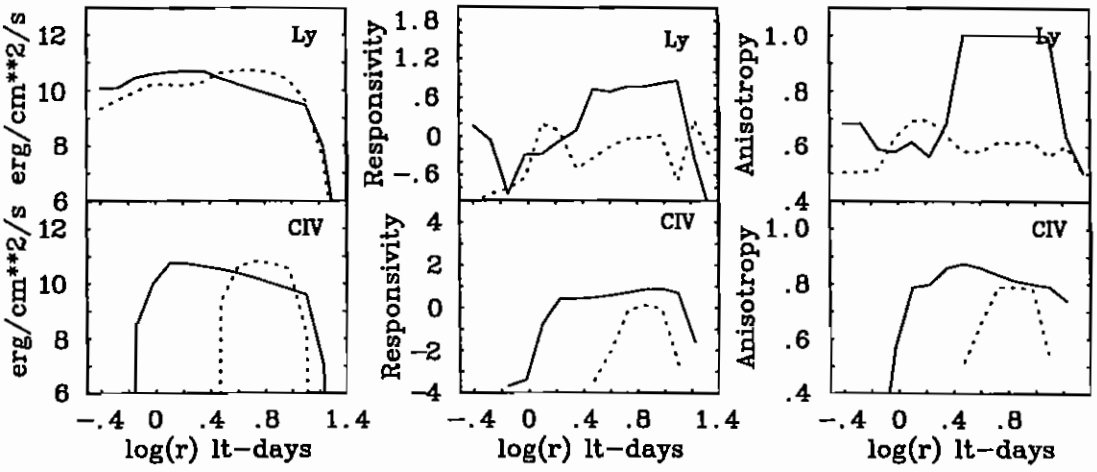

Fig. 13. The radial dependance of line emissivity, responsivity and the anisotropy factor in Model G. The (*full line*) data were obtained for low continuum luminosity and the (*dotted line*) data were obtained for high continuum luminosity.

especially at low redshifts. Wills *et.al.* (1993) have analysed the profile of the C IV line in a large sample of high redshift quasars. The profiles of the Lyα and C IV lines in low redshift quasars and AGNs have been investigated by Gondhalekar (1995). This study suggests that the profiles of these lines are very similar and symmetric, however, this study is based on *IUE* data and the low resolution of the *IUE* spectrographs ($\sim$1150 km s^{-1}) is a serious handicap for profile analysis.

A preliminary analysis of the changes in the profile of the C IV line observed in a small sub-sample of data obtained during the 1989 campaign to monitor NGC5548, has been presented by Crenshaw & Blackwell (1990). In this section the profile of the C IV line in NGC 5548, observed during the *IUE/HST* campaign of 1993 (Korista *et.al.* 1995), is investigated. The aim here is to identify the temporal variability of the profile; a detailed study of profile variability and the correlation of this variability with line and continuum parameters will be deferred to a later publication. The variability of the profile of the C IV line in the *IUE* and *HST* spectra obtained from Julian date (2440000+)9096.67 to Julian day 9135.12 is considered here (Korista *et.al.* 1995). In this analysis the NEWSIPS extraction of the *IUE* spectra has been used and the extraction and calibration of the *HST* data has been described by Korista *et.al.* (1995).

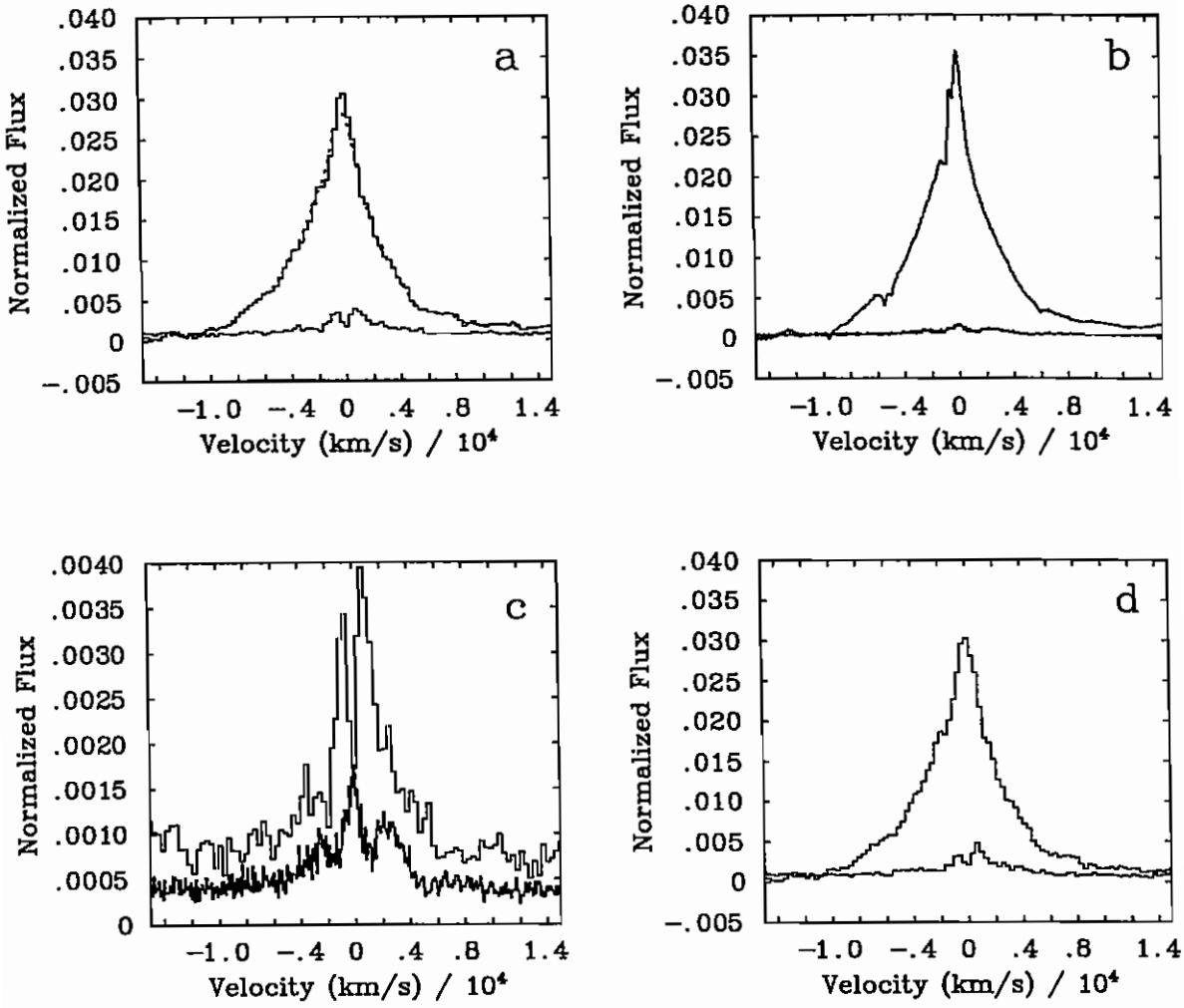

Fig. 14. The mean profile and the standard deviation profile of the C IV line in NGC5548. (a) *IUE* data (the degraded *HST* profile is superimposed (*dots*) and is just visible) and (b) *HST* data. (c) An expanded view of the standard deviation profiles obtained for *IUE* and *HST* data and (d) The mean profile and the standard deviation for the entire 1993 *IUE* campaign to monitor NGC5548 (see text for details)

In order to investigate the changes in the profile, the line profile was corrected for the underlying continuum and normalised as follows: (1) Both *IUE* and *HST* spectra were resampled on a uniform wavelength scale, a wavelength step of 1.70Å and 0.4Å was used for *IUE* and *HST* spectra respective-

ly. (2) The continuum level was obtained by fitting a straight line between 1375Å and 1800Å. These two wavelength points were selected because in the higher resolution and higher signal-to-noise ratio *HST* spectra the signal level is lowest at these two points. The mean continuum flux at these wavelengths was obtained by averaging data in two 25Å wide bands. The interpolated continuum was subtracted from the spectrum between 1375Å and 1800Å. (3) All spectra were then normalised to unit intensity of the C IV line measured between 1500Å and 1630Å. This form of normalisation preserves the profile of a line independent of the line intensity. (4) The wavelength scale was converted to velocity scale with zero at the peak of the C IV line. (5) A mean profile was created by averaging the normalised flux in each bin, between -15000 km s^{-1} to $+15000$ km s^{-1}, for all spectra. The flux in each bin was given equal weight to avoid a signal-to-noise bias. (6) The standard deviation was obtained for each bin. The 'standard deviation profile' is a measure of the change in the profile of a line. Unfortunately this measure is extremely sensitive to noise as this is added in quadrature. The fixed pattern noise in the *IUE* spectra is an additional 'noise'. Successive *IUE* spectra were obtained over the same part of the *IUE* camera and the fixed pattern noise also adds in quadrature in the the standard deviation profile.

The mean *IUE* and *HST* profiles of the C IV line in NGC 5548 are shown in Fig. 14a. and Fig. 14b. respectively. The higher resolution of the *HST* spectra is obvious from the absorption features in the blue wing of the profile. If the resolution of the *HST* profile is degraded with a Gaussian of FWHM = 6Å then the *HST* and *IUE* profiles are identical as can be seen from the superposition of the degraded *HST* profile on the *IUE* profile (Fig. 14a). The standard deviation profiles of the *IUE* and *HST* profiles are shown in Fig. 14c. The higher standard deviation in the *IUE* profile is due to higher noise in these spectra.

However, the general characteristics of these two standard deviation profiles are similar; the changes in the C IV profile are at velocities lower than $\sim$ 4000 km s^{-1} and are not symmetric, and there is little or no change at high velocities. In Fig. 14d. the mean profile and the standard deviation profile of the C IV line observed over the entire *IUE* monitoring campaign of 1993 (Korista *et.al.* 1995) has been shown, *i.e.* data obtained from Julian day (240000+)9060.64 to 9134.50. This mean profile is almost identical to the mean profile in the latter half of this campaign (Fig. 14a) although the continuum history of this profile is very different. The C IV line in NGC 5548 has an exceptionally robust profile and the kinematics of the BLR clouds does not change significantly even when the flux of ionizing radiation changes by a large fraction, so clearly the motion of the clouds is not influenced by the ionizing radiation.

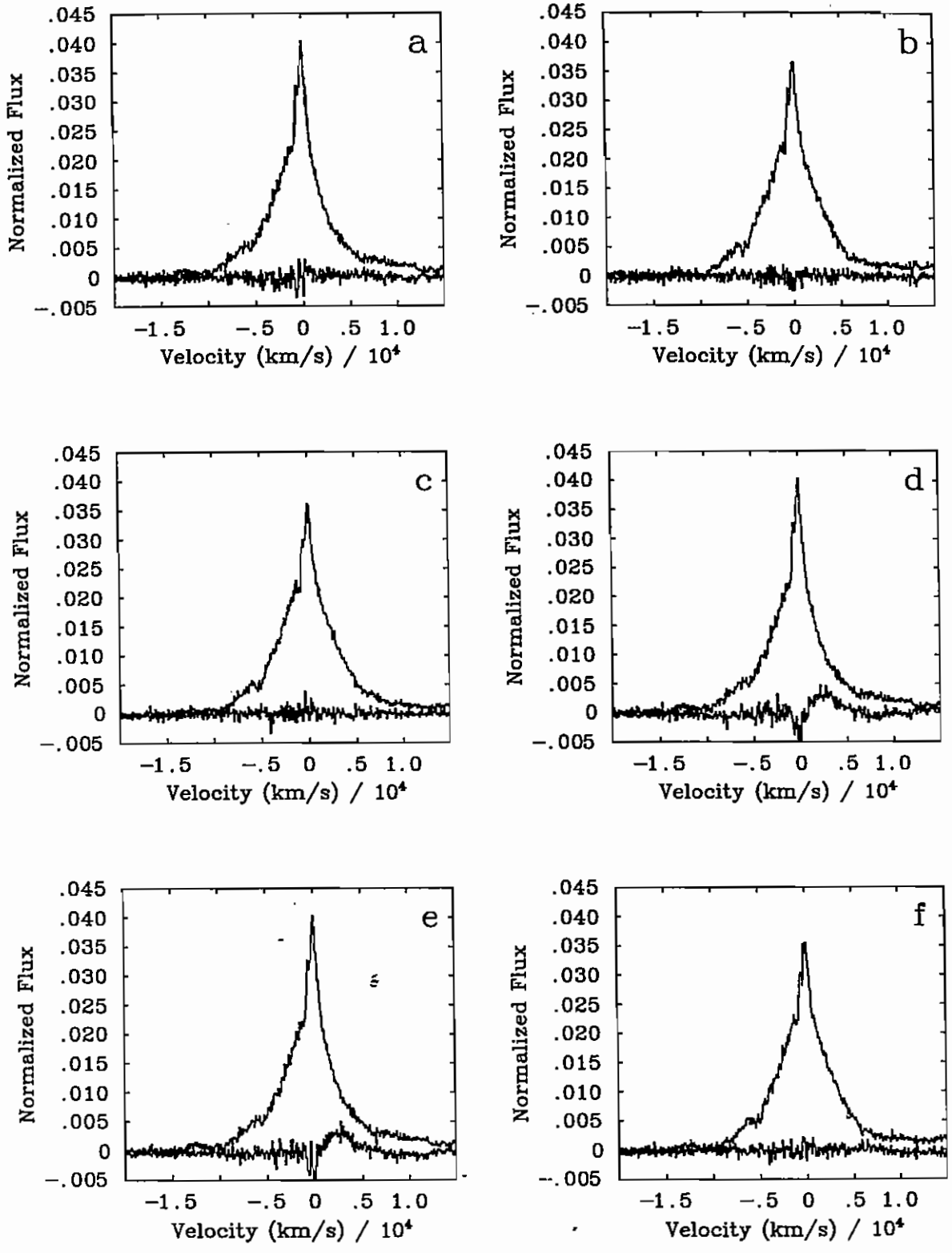

Fig. 15. The differenced profiles of C IV line in NGC5548. (a) profile in file n59097 and (n59098–n59097), (b) n59123 and (n59124–n59123), (c) n59134 and (n19135–n59134), (d) n59097 and (n59124–59097), (e) n59097and (n19135–n59097) and (f) n59123and (n19135–n59123). See Korista *et al.* (1995) for details of the IDs.

TABLE II
Data for Analysis of the Profile of the C IV line

File ID	JD(2440000+)	F_{1375}	$F_{C\,IV}$
n59097	9096.97	2.38	5.29
n59098	9098.10	2.56	5.14
n59123	9122.94	4.45	6.86
n59124	9123.00	4.28	6.95
n59134	9133.74	2.84	6.83
n59135	9135.12	2.80	6.62

ID see Korista *et.al.* (1995) for details of file ID
F_{1375} Mean Continuum at 1375Å
(10^{-14} erg cm^2 s^{-1} Å^{-1})
$F_{C\,IV}$ Integrated (from 1500Å to 1630Å)
intensity of the C IV line (10^{-12} erg cm^{-2} s^{-1})

The standard deviation profile is a measure of the change in the profile but it does not indicate the direction in which the changes have taken place. In order to investigate how the profiles vary, three sets of spectra from the beginning, end and middle of the *HST* monitoring campaign were selected (two spectra in each set). The spectra used, the continuum flux at 1375Å and the intensity of the C IV line in these spectra are given in Table 2. The C IV line in these spectra were corrected for the background and normalised as described above. The difference in the adjacent profiles is shown in Fig. 15a,b,c. These adjacent spectra were obtained about 24 hours apart and clearly the profile of the C IV line has not changed in this period, nor have the continuum and line luminosities changed over these 24 hr periods. The difference in the profile (n59124–n59097) (see Korista *et.al.* 1995, for details of the file nomenclature) is shown in Fig. 15d, and changes can now be seen around 0 km s^{-1} and up to +5000 km s^{-1} in the red-wing. Also subtle small changes can be seen at higher velocities in the red-wing and at low velocities in the blue-wing. Allowing for the delay between the core response relative to the line wings (Korista *et.al.*), these changes are consistent with the standard deviation profile in Fig. 14c. The red-wing feature is caused by the higher amplitude responsivity of the red wing as the continuum rises from a local

minimum. During this period of about 24 days the continuum luminosity increased by about a factor of two and the line luminosity increased by about 35%. The difference in the profile (n59135–n59097) is shown in Fig. 15e. Differences in the profiles similar to those shown in Fig. 15d can also be seen here. The continuum luminosities in spectrum n59097 and n59135 are similar but the line luminosity is still high by 35%. The difference in the profile (n59135–n59124) is shown in Fig. 15f; these two profiles are very similar. The observed changes in profile shape appear to be confined to the first half of the HST campaign.

5. Summary & Conclusions

In this paper the continuum energy distribution of NGC5548, from radio to gamma-ray energies, is described; this CED is based on observations as much as possible. The crucial ionizing continuum (from ~10 eV to ~2 keV) is determined by interpolating between observations at wavelengths longer than ~1200Å and observations at energies higher than ~150 eV. The ionizing continuum used in this paper is thus based firmly on observations. The covering factor of the BLR clouds is measured by equating the integrated ionizing continuum to the observed intensity of the Lyα line. The value of the covering factor for NGC5548 is ~0.18 and this is very similar to the covering factor of high redshift and high luminosity quasars (Smith *et.al.* 1981;Gondhalekar & Kellett 1995). It would appear that the covering factor of the BLR clouds in AGNs and quasars is independent of both redshift and luminosity.

Two models of the BLR in NGC5548 are described; these models differ in their physical structure but both models assume a spherical geometry. Both models can reproduce the luminosities of the HILs, except for O VI and N V, which are over-estimated. The centroid of the response functions of the HILs obtained from these models are in agreement with the centroids of the CCF. However, only model G can reproduce the observed correlation between the C IV/Lyα ratio and the continuum luminosity. This suggests that the column density of the region of the BLR where the Lyα and C IV lines are formed, can not be very high as the gas in this region must become optically thin for the excursions observed in the continuum of an AGN. The centroids of the HILs in this model are not a strong function of continuum luminosity.

Both model F and model G fail to reproduce the luminosities and centroids of the LILs, in both models the LIL luminosities are underestimated by a factor two to ten. This disagreement has variously been called the Lyα/Hβ problem (Baldwin 1978) and the energy balance problem (Netzer 1985). Gondhalekar & Kellett (1995) have shown that the ionizing contin-

uum of AGNs and quasars (similar to the ionizing continuum of NGC5548 used here) has enough photons to reproduce the observed luminosity of the Lyα line (for a covering factor of 0.2) but not that of the Hβ line if Case B conditions are assumed. This is similar to the results of Model F and G, and clearly suggests an additional source of energy for the BLR. If this energy input is by absorption of hard X-rays then the region of the BLR where the LILs are formed must have high column density clouds. The hard X-rays could be absorbed in an accretion disc as suggested by Collin-Souffrin *et.al.* (1986) (also see Rokaki 1995). It is equally possible that a BLR in which the density and column density increase with distance from the central source would meet the conditions required to reproduce the HILs and LILs from the same ensemble of clouds. Such models will be investigated in future publications.

The profile of the C IV line in NGC5548 is investigated during a period when both the continuum luminosity and the luminosity of the C IV line have increased by a large factor. Only very small changes, around the peak and in the red-wing of the line, have been observed. This suggests a very robust profile and the velocity structure of the BLR clouds is not affected by changes in the source luminosity.

In this paper an attempt has been made to model the BLR in NGC5548. It has not been possible to present a 'complete and final' model of the BLR in this AGN, but a number of aspects of the BLR have been identified which are necessary to bring modelled parameters in agreement with observations. These aspects would have to be built into future models of the BLR in AGNs and quasars.

Acknowledgements

This paper was produced with the facilities provided by the STARLINK Project, funded by PPARC. G.J. Ferland is thanked for providing a copy of the CLOUDY code and for assistance in using the code. PMG would like to thank B.M. Peterson and K.T. Korista for providing respectively the *IUE* and *HST* data obtained during the 1993 campaign to monitor NGC5548.

References

Baldwin J.A. : 1977, *Astrophysical Journal* **214**, 679
Bahcall J.N. Kozlovsky B.Z. : 1969, *Astrophysical Journal* **155**, 1077
Binette L., Prieto A., Szuszkiewicz E., Zheng W. : 1989, *Astrophysical Journal* **343**, 135
Blandford R.D., McKee C.F. : 1982, *Astrophysical Journal* **255**, 419
Boroson T.A., Green R.T. : 1992, *Astrophysical Journal, Supplement Series* **80**, 109

Cranshaw D.M., Blackwell J.H. : 1990, *Astrophysical Journal* **358**, L37
Clavel J., Santos-Lleó M. : 1990, *A& A* **230**, 3
Clavel J., *et.al.* : 1991, *Astrophysical Journal* **366**, 64
Collin-Souffrin S., Dumont S., Joly M., Péquignot D. : 1986, *A& A* **166**, 27
Davidson K. : 1972, *Astrophysical Journal* **218**, 20
Davidson K., Netzer H. : 1979, *Rev. Mod. Phys.* **51**, 715
Dietrich, M., *et.al.* : 1993, *Astrophysical Journal* **408**, 416
Ferland G.J., Persson S.E. : 1989, *Astrophysical Journal* **347**, 656
Ferland G.J., Peterson B.M., Horne K., Welsh W.F., Nahar S.N. : 1992, *Astrophysical Journal* **387**, 95
Ferland G.J. : 1993, *HAZY*, University of Kentucky, Department of Physics & Astronomy; Internal Report,
Gaskell C.M., Sparke L.S. : 1986, *Astrophysical Journal* **305**, 175
Gaskell C.M., Peterson B.M. : 1987, *Astrophysical Journal, Supplement Series* **65**, 1
Goad M.R., O'Brien P.T., Gondhalekar P.M.: 1993, *Monthly Notices of the RAS* **263**, 149 (Paper I)
Goad M.R. : 1995, *Ph.D Thesis*, University of London
Gondhalekar P.M., Wilson R. : 1980, *Nature* **285**, 461
Gondhalekar P.M. : 1992, *Monthly Notices of the RAS* **255**, 663
Gondhalekar P.M. : 1995, *Monthly Notices of the RAS* , submitted
Gondhalekar P.M. & Kellett B.J. : 1994, 'The Ionizing Continuum in AGNs and Quasars' in Gondhalekar P.M., Horne K., & Peterson B.M., ed(s)., *Reverberation Mapping of the Broad-Line Region In Active Galactic Nuclei*, Astronomical Society of the Pacific: San Francisco, 241
Grevesse N., Anders E. : 1989, 'No. 183, Cosmic Abundance of Matter' in Waddington C.J., ed(s)., , AIP: New York,
Hamann F., Ferland G.J. : 1993, *Astrophysical Journal* **418**, 11
Horne K., Welsh W.F., Peterson B.M. : 1991, *Astrophysical Journal* **367**, L5
Jourdain E., *et.al.* : 1992, *A& A* **256**, L38
Kinney A.L., Rivolo A.R., Koratkar A.P. : 1990, *Astrophysical Journal* **357**, 338
Korista K.T., *et.al.* : 1995, *Astrophysical Journal, Supplement Series* **97**, 285
Kwan J., Krolok J.H. : 1981, *Astrophysical Journal* **250**, 478
MacAlpine G.M. : 1972, *Astrophysical Journal* **175**, 11
Maoz D., *et.al.*: 1993, *Astrophysical Journal* **404**, 576
Maoz D. : 1994, 'Echo Mapping of the BLR - A Critical Appraisal' in Gondhalekar P.M., Horne K., & Peterson B.M., ed(s)., *Reverberation Mapping of the Broad-Line Region In Active Galactic Nuclei*, Astronomical Society of the Pacific: San Francisco, 95
Mathews W.G., Ferland G.J. : 1987, *Astrophysical Journal* **323**, 456
Netzer H. : 1985, *Astrophysical Journal* **289**, 415
Netzer H. : 1990, 'AGN Emission Lines' in Courvoisier, T.J.-L., & Mayor, M., ed(s)., *Active Galactic Nuclei*, Springer: Saas-Fee Advanced Course 20,
Neugebauer G., Oke J.B., Becklin E.E., Matthews K. : 1979, *Astrophysical Journal* **230**, 79
O'Brien P.T., Goad M.R., Gondhalekar P.M. : 1994, *Monthly Notices of the RAS* **268**, 845 (Paper II)
O'Brien P.T., Goad M.R., Gondhalekar P.M. : 1995, *Monthly Notices of the RAS* , submitted (Paper III)
Osterbrock D. : 1993, *Astrophysical Journal* **404**, 551
Penston M.V., *et.al.* : 1981, *Monthly Notices of the RAS* **196**, 857
Penston M.V. : 1991, 'The Trouble with Reverberation' in Miller H.R., & Wiita P.J., ed(s)., *Variability of Active Galactic Nuclei*, Cambridge Univ. Press: Cambridge, 343
Pérez E., Robinson A.R., de la Fuente L. : 1992a, *Monthly Notices of the RAS* **255**, 502
Pérez E., Robinson A.R., de la Fuente L. : 1992b, *Monthly Notices of the RAS* **256**, 103
Peterson B.M., *et.al.* : 1991, *Astrophysical Journal* **366**, 119
Peterson B.M. : 1993, *Publications of the ASP* **105**, 247

Peterson B.M. : 1994, 'An Overview of Reverberation Mapping: Progress and Problems' in Gondhalekar P.M., Horne K., & Peterson B.M., ed(s)., *Reverberation Mapping of the Broad-Line Region In Active Galactic Nuclei*, Astronomical Society of the Pacific: San Francisco, 1

Pogge R.W., Peterson B.M. : 1992, **103**, 1084

Rees M.J., Netzer H., Ferland G.J. : 1989, *Astrophysical Journal* **347**, 640

Robinson A. : 1994, 'The LAG Spectroscopic Monitoring Campaign: An Overview' in Gondhalekar P.M., Horne K., & Peterson B.M., ed(s)., *Reverberation Mapping of the Broad-Line Region In Active Galactic Nuclei*, Astronomical Society of the Pacific: San Francisco, 147

Rokaki E. : 1994, 'Reverberation and the Disk Model of AGN' in Gondhalekar P.M., Horne K., & Peterson B.M., ed(s)., *Reverberation Mapping of the Broad-Line Region In Active Galactic Nuclei*, Astronomical Society of the Pacific: San Francisco, 257

Smith M.G., *et.al.* : 1981, *Monthly Notices of the RAS* **195**, 437

Shields J.C., Ferland G.J., Peterson B.M. : 1995, *Astrophysical Journal* **441**, 507

Ulrich M.H., *et.al.* : 1980, *Monthly Notices of the RAS* **192**, 561

Wamsteker W., Colina L. : 1986, *Astrophysical Journal* **311**, 617

Walter R., *et.al.* : 1994, *A&A* **285**, 119

White R.J., Peterson B.M. : 1994, *Publications of the ASP* **106**, 879

Zheng, W., Kriss, G.A., Davidsen, A.F. : 1995, *Astrophysical Journal* **440**, 606